

Fusion of necklace-ring patterns into vortex and fundamental solitons in dissipative media

Y. J. He,^{1,2} Boris A. Malomed,³ and H. Z. Wang^{1,*}

¹*State Key Laboratory of Optoelectronic Materials and Technologies,
Zhongshan (Sun Yat-Sen) University, Guangzhou 510275, China*

²*School of Electronic and Information Engineering,
Guangdong Polytechnic Normal University, Guangzhou 510665, China*

³*Department of Interdisciplinary Studies,
School of Electrical Engineering, Faculty of Engineering,
Tel Aviv University, Tel Aviv 69978, Israel*

Abstract

We demonstrate that necklace-shaped arrays of localized spatial beams can merge into stable fundamental or vortex solitons in a generic model of laser cavities, based on the two-dimensional complex Ginzburg-Landau equation with the cubic-quintic nonlinearity. The outcome of the fusion is controlled by the number of "beads" in the initial necklace, $2N$, and its topological charge, M . We predict and confirm by systematic simulations that the vorticity of the emerging soliton is $|N - M|$. Threshold characteristics of the fusion are found and explained too. If the initial radius of the array (R_0) is too large, it simply keeps the necklace shape (if R_0 is somewhat smaller, the necklace features a partial fusion), while, if R_0 is too small, the array disappears.

PACS numbers: 42.65.Tg, 42.65.Jx

Keywords: necklace-ring patterns, fundamental solitons, vortex solitons

*Corresponding author, E-mail: stswzh@mail.sysu.edu.cn

I. INTRODUCTION

The complex Ginzburg-Landau (CGL) equation is a universal model which plays an important role in many areas such as in superconductivity and superfluidity, fluid dynamics, reaction-diffusion phenomena, nonlinear optics, Bose-Einstein condensation, and quantum field theories [1, 2, 3]. The CGL models produce dynamical behaviors, e.g., spatiotemporal chaos and formation of periodic patterns to dissipative solitons and their bound states [1, 2, 3, 4, 5].

Many recent works focused on localized complex patterns in conservative models of optical media, different from the simplest nodeless ground-state modes, such as vortex solitons [6], soliton clusters [7, 8], dipole-mode structures and their multipole counterparts [9, 10, 11, 12, 13], and necklace-ring solitons (NRSs) [14, 15, 16]. Similar patterns may be stable in dissipative models based on the CGL equation with the cubic-quintic (CQ) nonlinearity. These include stable localized vortices in two- and three-dimensional (2D and 3D) CGL equation [17, 18, 19] and necklace-shaped soliton clusters [20]. Recently, stable spatiotemporal NRSs were also reported in the 3D CQ-CGL equation [21].

Previous studies of complex dissipative-solitons patterns were focused on their stability. A more general issue is a possibility of dynamical transformation (fusion) of an initial soliton cluster into complex structures of a different type, or into a simple fundamental soliton. In this work, we demonstrate that necklace patterns can fuse into stable fundamental and vortex dissipative solitons in the 2D CQ complex GL equation, which is controlled by topological numbers of the initial pattern. Such an outcome is only possible in dissipative models, where the energy and angular momentum are not dynamical invariants. We predict the vorticity of the eventual state, and corroborate it by numerical results. If the initial radius of the necklace array is too large, it features a partial fusion, or simply keeps the initial structure; on the other hand, if the initial radius is too small, the pattern decays to zero.

II. THE MODEL

Following the notation adopted in Ref. [17], we consider the CGL equation with the CQ nonlinearity in the (2+1)-dimensional setting, with propagation distance Z and transverse coordinates, X and Y :

$$iu_Z + i\alpha u + (1/2 - i\beta)(u_{XX} + u_{YY}) + (1 - i\varepsilon)|u|^2u - (\nu - i\mu)|u|^4u = 0, \quad (1)$$

where $\alpha > 0$ and $\mu > 0$ are parameters of the linear and quintic loss (the latter one accounts for the gain saturation), $\varepsilon > 0$ is the cubic gain, ν (that may be both positive and negative) accounts for the quintic self-defocusing/focusing, the diffraction and cubic self-focusing coefficients are normalized to be 1, and $\beta > 0$ is the effective diffusion coefficient. Except for the latter one, all other coefficients are standard ingredients of optical models based on the CGL equations; as for β , it appears in models of laser cavities, as [22] $\beta = -\tau_p\tau_c\Delta/(\tau_p + \tau_c)^2$ (in normalized units), where τ_p and τ_c are the polarization-dephasing and cavity-decay times, and Δ detuning between the cavity's and atomic frequencies. Therefore, the relevant case of $\beta > 0$ corresponds to the negative detuning.

We stress that the CQ nonlinearity in Eq. (1) is not a truncated expansion of a saturable nonlinearity, but represents a fundamental response of the nonlinear medium, due to some intrinsic resonance(s) in it. This response was directly observed in chalcogenide glasses [23, 24] and in some organic optical materials [25], although saturable nonlinearity is more generic in optics [2].

The model based on the CGL equation (1) does not take into regard the finite relaxation time of the gain and loss in optical media, which may be added to the model through the respective evolution equation [2, 26, 27]. However, it seems quite plausible that the results reported below will not be strongly affected by this modification of the model.

It has been demonstrated that vortex solitons and soliton clusters can self-trap in the framework of the 2D CQ-CGL model (and its 3D extension), provided that coefficient β is presented [17, 18, 19, 20, 21]. The stability of the localized patterns is supported by the simultaneous balance between the transverse diffraction and self-focusing, and between the gain and linear and quintic losses (including the effective diffusive loss, accounted for by $\beta > 0$).

Following Refs. [14, 15, 16], the initial necklace-shaped pattern, with amplitude A , mean radius R_0 , and width w , can be taken (in polar coordinates r and θ) as

$$u(Z = 0, r, \theta) = A \operatorname{sech}[(r - R_0)/w] \cos(N\theta) \exp(iM\theta), \quad (2)$$

Here, integer N determines the number of elements ("beads") in the ring (necklace) structure, which is $2N$, while another integer, M , is the topological charge of the complex pattern.

III. NUMERICAL RESULTS

Analysis of numerical results demonstrates that generic outcomes of the evolution of the necklace array can be displayed, e.g., for $\alpha = 0.5$, $\beta = 0.5$, $\varepsilon = 2.5$, $\nu = 0.01$, and $\mu = 1$, which corresponds to a physically realistic situation and, simultaneously, makes the evolution relatively fast, thus helping to elucidate its salient features [15, 18, 19]. In this case, the amplitude and width of the individual 2D stable fundamental soliton, as found from Eq. (1), are $A = 1.6$ and $w = 1$. The robustness of the emerging patterns was tested in direct simulations of Eq. (1) with the initial condition taken as expression (2) additionally multiplied by $[1 + \rho(x)]$ where $\rho(x)$ is a Gaussian random function with zero average, the mean size of the perturbation amounting to 10 percent of the soliton's amplitude.

The array with the topological charge equal to half the number of "beads" in the necklace, i.e., $M = N$, merges into a fundamental soliton, under the condition that initial radius R_0 of the necklace array is smaller than a certain critical value, R_{max}^F , see Fig. 1(a). As follows from Eq. (2), the mean phase shift between adjacent beads in the initial array is $\Delta\varphi = \Delta\varphi_0 + 2\pi M/(2N) = 0$, where $\Delta\varphi_0 = -\pi$ corresponds to the opposite sign of adjacent "beads" in the necklace with $M = 0$. Therefore, individual elements in the array, being in-phase, attract each other, which leads to their fusion into a stable fundamental soliton, as seen in Figs. 1(b, c).

Note that the CGL equation, being a dissipative one, does not have any dynamical invariant, hence the total angular momentum is not conserved either. In fact, the initial configuration corresponding to Eq. (2) with $M = N$ may be realized as a mixture of two states, with values of the vorticity (total topological charge) $S = M - N \equiv 0$ and $S = M + N$. Obviously, the effective diffusion term in underlying Eq. (1), which is proportional to β , produces a much stronger dissipation effect on the component of the wave field with the nonzero vorticity, hence only the zero-vorticity one survives in the limit of $Z \rightarrow \infty$, as observed in Fig. 1.

It is also easy to understand the increase of R_{max}^F with N , see Fig. 1(a). Indeed, the attraction between adjacent "beads", necessary for their fusion into the fundamental soliton,

is not too weak if the separation between them does not exceed a certain (maximum) value [5]. The radius of the necklace, corresponding to a given separation between the "beads", grows linearly with N , which explains the roughly linear form of dependence $R_{max}^F(N)$ in Fig. 1(a).

When radius R_0 of the initial necklace pattern is larger than a certain minimum value, R_{min}^V , but smaller than $1.8N$, i.e.,

$$R_{min}^V \leq R_0 \leq 1.8N, \quad (3)$$

the array with topological charge M evolves into a stable vortex soliton, provided that M falls into either of two mutually symmetric intervals, $M_{min}^V \leq M < N$ or $N < M < M_{max}^V \leq 2N - M_{min}^V$ see Fig. 2. As said above, initial configuration (2) may be realized as a mixture of states with vorticities whose absolute values are $S = |N \pm M|$, hence the vorticity component which may survive in the course of the evolution (one which is least affected by the diffusion term) is $S_{fin} = |N - M|$. Indeed, the simulations confirm that the emerging vortex soliton features precisely this value of the vorticity. Because the asymptotic form of the vortex at $r \rightarrow 0$ is $\text{const} \cdot r^S$, smaller values of $S \equiv |N - M|$ correspond to a smaller radius of the inner hole in the vortex soliton, as observed in Figs. 2(c-e). Dependence $M_{min}^V(R_0)$, which is displayed in Fig. 2(b) for fixed values of N , can be explained too. Indeed, well-pronounced minima in the dependence at intermediate values of R_0 corresponds to the fact that the fusion of the necklace array into vortex soliton is most feasible when the initial radius of the pattern is close to the radius of the expected vortex ring, which determines the location of the minima in Fig. 2(b).

On the other hand, when the initial radius of the necklace is smaller than the minimum value, R_{min}^V [see Eq. (3)], the pattern rapidly disappears (decays to zero) upon the propagation, irrespective of the value of M , as shown in Fig. 2(f). This effect is explained by the strong dissipation generated by the effective diffusion term in Eq. (1) (the one proportional to β) in the necklace array of a small radius. Naturally, the diffusive dissipation is stronger for a larger azimuthal gradient. The latter grows, on the average, linearly with N , that is why R_{min}^V also increases with N , as seen in Fig. 2(a).

If the initial radius of the necklace exceeds the above-mentioned maximum values, i.e., for the case of $M = N$, and $\approx 1.8N$ for $M \neq N$, as per Eq. (3) (recall these two cases correspond to the fusion of the necklace into the fundamental and vortex soliton, respectively), Fig. 3

shows that the necklace arrays with $M = 0$ do not undergo the fusion, but feature slow expansion, while their counterparts with $M \neq 0$ make the number of the "beads" smaller via the fusion involving some of them, after passing several hundred diffraction lengths. The number of the lost "beads" is larger for smaller values of $|M - N|$, and smaller initial radius of the necklace, R_0 .

Finally, if the initial radius exceeds a still larger threshold value, R_{min}^N , the interaction between the "beads" in the necklace array becomes negligible, irrespective of its topological charge M (which implies R_{min}^N is defined with some uncertainty, as it may slightly vary with the change of the total propagation distance). As a result, the pattern keeps its necklace-like structure and the initial radius, as shown in Fig. 4. For the same reasons as mentioned above [cf. Fig. 1(a)], the dependence of the respective minimum radius R_{min}^N on modulation number N of initial pattern (2) is approximately linear, see Fig. 4(a). Note that each individual element in the necklace patterns observed in Figs. 4 features an isotropic (circular) shape, unlike the "beads" in the initial pattern. This is explained by the fact that each element evolves into a fundamental soliton, whose deformation induced by the interaction with its neighbors is negligible, since the distance to them is too large. In fact, the "freezing" of soliton necklaces of a large radius due to the exponential decay of the interaction forces was observed in many cases before [15, 16?].

IV. CONCLUSION

We have demonstrated that, unlike conservative systems described by multidimensional nonlinear Schrödinger equations, models of dissipative optical media (in particular, laser cavities [22]), based on the 2D CGL equation with the cubic-quintic nonlinearity, admit fusion of necklace-ring patterns into stable fundamental and vortical solitons, provided that the initial radius of the ring, R_0 , is not too large (if R_0 is somewhat larger, the necklace may undergo a partial fusion). The outcome of the evolution is controlled by values of modulation number N and topological charge M of initial necklace (2). A simple analysis has predicted the vorticity of the fused soliton to be $|N - M|$, which is fully confirmed by direct simulations. Threshold characteristics of the fusion process, such as those displayed in Figs. 1(a) and 2(a, b), were also explained in a qualitative form. The possibility to control the outcome of the fusion by means of the initial topological numbers, N and M , suggests a

principal possibility to use the process in all-optical switching schemes. On the other hand, if the initial radius of the necklace array is too large, the interaction between individual elements is negligible, allowing the pattern to keep its initial radius and necklace structure, while each element assumes the isotropic shape, corresponding to fundamental dissipative solitons in 2D.

In addition to the straightforward realizations in terms of nonlinear optics, the model may also find application to Bose-Einstein condensates, where the dissipation and gain occur in models of matter-wave lasers, as demonstrated experimentally and theoretically in various settings [28, 29, 30, 31, 32, 33, 34, 35, 36, 37]. Thus far, such models were analyzed only in the effectively 1D geometry, while the present results suggest to extend them into two dimensions.

V. ACKNOWLEDGEMENTS

This work was supported by the National Natural Science Foundation of China (10674183) and National 973 Project of China (2004CB719804), and Ph. D. Degrees Foundation of Ministry of Education of China (20060558068).

-
- [1] I. S. Aranson and L. Kramer, *Rev. Mod. Phys.* **74**, 99(2002).
 - [2] N. N. Rosanov, (Springer-Verlag, 2002).
 - [3] B. A. Malomed, *Encyclopedia of Nonlinear Science*, pp. 157, ed. by A. Scott (Routledge, New York, 2005); *Chaos* **17**, 037117 (2007).
 - [4] N. Akhmediev and A. Ankiewicz, *Lecture Notes in Physics Vol. 661* (Springer, Berlin, 2005).
 - [5] B.A. Malomed, *Phys. Rev. A* **44**, 6954 (1991).
 - [6] Z. Chen, H. Martin, E. D. Eugenieva, J. Xu, and J. Yang, *Opt. Express* **13**, 1816 (2005).
 - [7] A. S. Desyatnikov and Yu. S. Kivshar, *Phys. Rev. Lett.* **88**, 053901 (2002).
 - [8] Y. V. Kartashov, L.-C. Crasovan, D. Mihalache, and L. Torner, *Phys. Rev. Lett.* **89**, 273902 (2002).
 - [9] J. J. Garcia-Ripoll, V. M. Perez-Garcia, E. A. Ostrovskaya, and Y. S. Kivshar, *Phys. Rev. Lett.* **85**, 82-85 (2000).

- [10] D. Neshev, W. Krolikowski, D. E. Pelinovsky, G. McCarthy, and Y. S. Kivshar, *Phys. Rev. Lett.* **87**, 103903 (2001).
- [11] T. Carmon, R. Uzdin, C. Pigier, Z. H. Musslimani, M. Segev, and A. Nepomnyashchy, *Phys. Rev. Lett.* **87**, 143901 (2001).
- [12] Y. V. Kartashov, R. Carretero-Gonzalez, B. A. Malomed, V. A. Vysloukh, and L. Torner, *Opt. Express* **13**, 10703 (2005).
- [13] Y. J. He and H. Z. Wang, *Opt. Express* **14**, 9832 (2006).
- [14] M. Soljačić, S. Sears, and M. Segev, *Phys. Rev. Lett.* **81**, 4851 (1998); *ibid.* **86**, 420 (2001).
- [15] D. Mihalache, D. Mazilu, L.-C. Crasovan, B. A. Malomed, F. Lederer, and L. Torner, *Phys. Rev. E* **68**, 046612 (2003).
- [16] J. Yang, I. Makasyuk, P. G. Kevrekidis, H. Martin, B. A. Malomed, D. J. Frantzeskakis, and Z. Chen, *Phys. Rev. Lett.* **94**, 113902 (2005).
- [17] L.-C. Crasovan, B. A. Malomed, and D. Mihalache, *Phys. Rev. E* **63**, 016605 (2001).
- [18] D. Mihalache, D. Mazilu, F. Lederer, Y. V. Kartashov, L.-C. Crasovan, L. Torner, and B. A. Malomed, *Phys. Rev. Lett.* **97**, 073904 (2006).
- [19] D. Mihalache, D. Mazilu, F. Lederer, H. Leblond, and B. A. Malomed, *Phys. Rev. A* **75**, 033811 (2007); *ibid.* **A 76**, 045803 (2007).
- [20] D. V. Skryabin and A.G. Vladimirov, *Phys. Rev. Lett.* **89**, 044101 (2002).
- [21] Y. J. He, H. H. Fan, J. W. Dong, and H. Z. Wang, *Phys. Rev. E* **74**, 016611 (2006).
- [22] J. Lega, J. V. Moloney, and A. C. Newell, *Phys. Rev. Lett.* **73**, 2978 (1994).
- [23] F. Smektala, C. Quemard, V. Couderc, and A. Barthelemy, *J. Non-Cryst. Solids* **274**, 232 (2000).
- [24] G. Boudebs, S. Cherukulappurath, H. Leblond, J. Troles, F. Smektala, and F. Sanchez, *Opt. Commun.* **219**, 427 (2003).
- [25] C. Zhan, D. Zhang, D. Zhu, D. Wang, Y. Li, D. Li, Z. Lu, L. Zhao, and Y. Nie, *J. Opt. Soc. Am. B* **19**, 369-375 (2002).
- [26] N. N. Rosanov, S. V. Fedorov, and A. N. Shatsev, *JETP* **102**, 547 (2006); *Phys. Rev. Lett.* **95**, 053903 (2005).
- [27] S. V. Fedorov, N. N. Rosanov, and A. N. Shatsev, *Optical Spectr.* **102**, 449 (2007).
- [28] B. A. Malomed, *Phys. Rev. E* **58**, 7928 (1998).
- [29] B. Kneer, T. Wong, K. Vogel, W. P. Schleich, and D. F. Walls, *Phys. Rev. A* **58**, 4841 (1998).

- [30] H. J. Miesner, D. M. Stamper-Kurn, M. R. D. S. Durfee, S. Inouye, and W. Ketterle, *Science* **279**, 1005 (1998).
- [31] E. W. Hagley, L. Deng, M. Kozuma, J. Wen, K. Helmerson, S. L. Rolston, and W. D. Phillips, *ibid.* **283**, 1706 (1999).
- [32] P. D. Drummond, K. V. Kheruntsyan and H. He, *J. Opt. B - Quant. Semicl. Opt.* **1**, 387 (1999).
- [33] D. Schneble, Y. Torii, M. Boyd, E. W. Streed, D. E. Pritchard, and W. Ketterle, *Science* **300**, 475 (2003).
- [34] L. D. Carr and J. Brand, *Phys. Rev. A* **70**, 033607 (2004).
- [35] M. I. Rodas-Verde, H. Michinel, and V. M. Prez-Garca, *Phys. Rev. Lett.* **95**, 153903 (2005).
- [36] P. Y. P. Chen and B. A. Malomed, *J. Phys. B - At. Mol. Opt. Phys.* **38**, 4221 (2005); *ibid.* **39**, 2803 (2006).
- [37] A. V. Carpentier, H. Michinel, M. I. Rodas-Verde, and V. M. Perez-Garcia, *Phys. Rev. A* **74**, 013619 (2006).

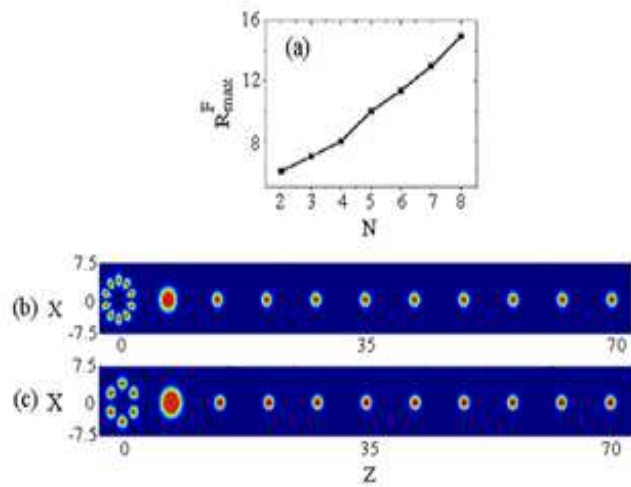


FIG. 1: (Color online) The fusion into a fundamental soliton of the necklace array whose initial radius is not too large, $R_0 \leq R_{amx}^F$, and the topological charge is equal to half the number of "beads" in the array, $M = N$. (a): The largest radius, admitting the fusion, versus N . (b, c): Examples of the fusion for $R_0 = 4$ and $M = N = 5$ (b) or $M = N = 3$ (c) [the examples are shown by means of contour plots of the local power, $|u(x, y)|^2$].

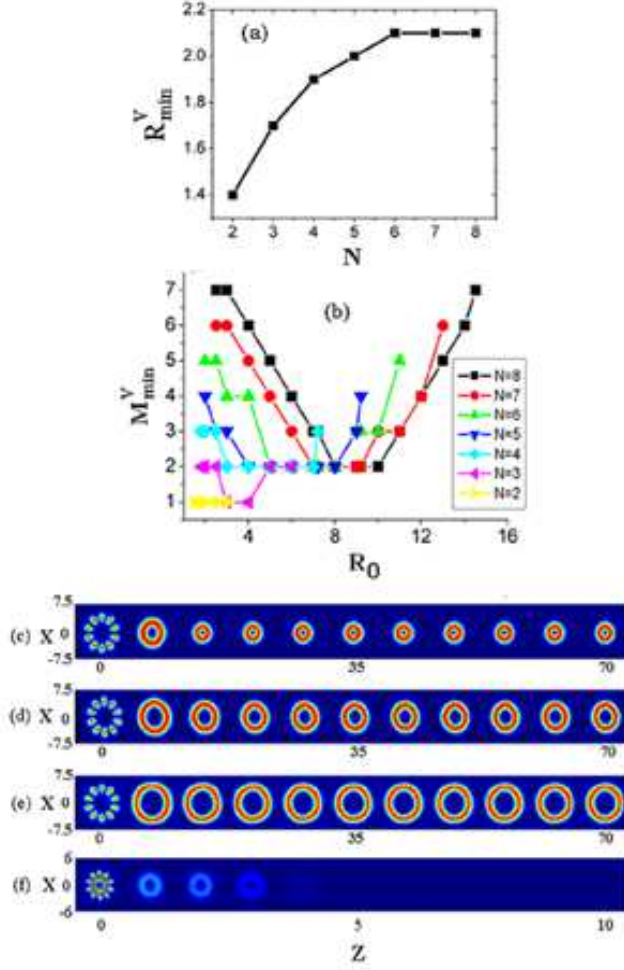


FIG. 2: (Color online) The fusion into a stable vortex soliton of the necklace whose initial radius and topological charge satisfy constraints $R_{min}^V \leq R_0 \leq 1.8N$, and either $M_{min}^V \leq M < N$ or $N < M < M_{max}^V \leq 2N - M_{min}^V$. (a): The minimum initial radius admitting the fusion versus N ; (b): the minimum topological charge versus the initial radius for different fixed values of modulation number N . (c-e): Examples of the formation of the vortex soliton with $N = 5$ and $R_0 = 5$ for $M = 4$ (c), $M = 3$ (d), and $M = 2$ (e). Additionally, panel (f) displays an example of the decay of the necklace cluster with $N = 5$ and $M = 4$, in the case of $R_0 < R_{min}^V$ (here, $R_0 = 1.9$ and $R_{min}^V = 2$).

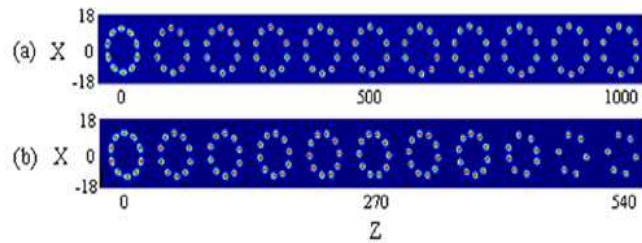


FIG. 3: (Color online) (a): Slow expansion of the necklace array with $N = 5$, $M = 0$ and $R_0 = 11$, in the case when its initial radius slightly exceeds the maximum value $1.8N$, see Eq. (3). (b): In the same case, but with $M = 3$, ten initial "beads" fuse into eight and, eventually, into six individual elements.

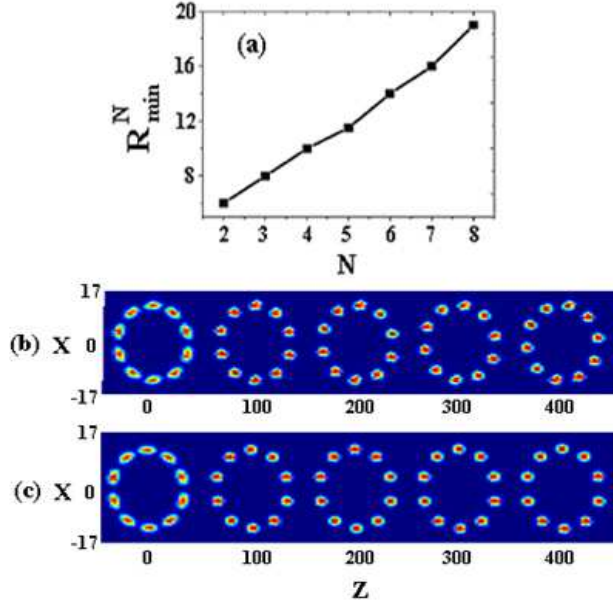


FIG. 4: (Color online) Formation of "frozen" patterns which look like stable soliton necklaces, with the initial necklace radius exceeding R_{min}^N and an arbitrary value of the topological charge (M). (a): R_{min}^N as a function of modulation number N (b, c): Examples of the formation of stable necklace rings with $N = 5$ and $R_0 = 12$ for $M = 2$ (b) and $M = 0$ (c).